Accepted Article

Title: Stabilization of the Reductase Domain in the Catalytically Self-Sufficient Cytochrome P450BM3 via Consensus-Guided Mutagenesis

Authors: GLORIA SAAB-RINCON, Hanan Alwaseem, Valeria Guzmán-Luna, Leticia Olvera, and Rudi Fasan

A Journal of

ChemPubSoc
Europe

WILEY-VCH   www.chembiochem.org

Stabilization of the Reductase Domain in the Catalytically Self-Sufficient Cytochrome P450$_{BM3}$ via Consensus-Guided Mutagenesis

Gloria Saab-Rincón*[a], Hanan Alwaseem[b], Valeria Guzmán-Luna[a], Leticia Olvera[a] and Rudi Fasan[b]

Abstract: The multi-domain, catalytically self-sufficient cytochrome P450 BM-3 from *Bacillus megaterium* (P450$_{BM3}$) constitutes a versatile enzyme for the oxyfunctionalization of organic molecules and natural products. However, the limited stability of the diflavin reductase domain limits the utility of this enzyme for synthetic applications. In this work, a consensus-guided mutagenesis approach was applied to enhance the thermal stability of the reductase domain of P450$_{BM3}$. Upon phylogenetic analysis of a set of distantly related P450s (% identity > 38%), a total of 14 amino acid substitutions were identified and evaluated in terms of their stabilizing effect relative to the wild-type reductase domain. Recombination of the six most stabilizing mutations resulted in the generation of two thermostable variants featuring up to 10-fold longer half-lives at 50°C and increased catalytic performance at elevated temperature. Further characterization of the engineered P450$_{BM3}$ variants indicated that the introduced mutations increase the thermal stability of the FAD-binding domain and that the optimal temperature (T$_{opt}$) of the enzyme has shifted from 25°C to 40°C. This work demonstrates the effectiveness of consensus mutagenesis for enhancing the stability of the reductase component of a multi-domain P450. The stabilized P450$_{BM3}$ variants developed here could potentially provide more robust scaffolds for the engineering of oxidation biocatalysts.

Introduction

Cytochrome P450s are heme-containing enzymes implicated in a broad range of oxidation processes as part of biosynthetic and xenobiotic metabolism pathways.[1] The ability of these enzymes to oxidize unactivated aliphatic C−H bonds makes them particularly attractive from a synthetic and biotechnological standpoint.[2] Within this enzyme superfamily, the fatty acid hydroxylase P450 BM-3 from *Bacillus megaterium* (P450$_{BM3}$) has attracted particular attention due to its 'catalytic self-sufficiency', resulting from the heme monooxygenase domain being directly

fused to a reductase domain.[3] In this enzyme, the reductase domain consists of three nucleotide-binding domains: a flavin mononucleotide (FMN) binding domain, a flavin dinucleotide (FAD) binding domain, and a nicotinamide adenine dinucleotide (NADPH) binding domain. Through the reductase domain, two electrons are transferred from the NADPH cofactor to the FAD domain and then to the FMN domain, from which electrons are supplied to the heme domain to support catalysis.[4]

Because of its single-polypeptide structure and high catalytic activity in fatty acid oxidation, P450$_{BM3}$ has been the object of extensive protein engineering efforts[5] in order to alter its substrate profile for the oxidation of small organic molecules,[6] synthesis of drug metabolites,[7] diversification of natural products,[8]; and production of biofuels.[9] Efforts toward increasing the thermal stability of this enzyme have also been reported and they have mostly focused on the isolated heme domain of P450$_{BM3}$,[10] which can function as a peroxygenase. [10] Since NADPH-driven oxidation catalysis with this enzyme is generally more efficient than that driven by H$_2$O$_2$, engineering efforts would greatly benefit from the availability of more stabilized forms of P450$_{BM3}$ holoenzyme. Previous studies indicated that the thermostability of this P450 is dictated by the reductase domain, which exhibits significantly lower stability compared to the heme domain (T$_m$: 48ºC vs. 63ºC, respectively).[11] With the goal of obtaining more stable P450$_{BM3}$ variants, Urlacher and coworkers constructed a chimera by combining the heme domain of P450$_{BM3}$ and the more stable reductase domain from the homologous CYP102A3 from *Bacillus subtilis*.[12] The chimeric enzyme was shown to exhibit a 10-fold longer half-life (8→100 min) at 50 °C but its catalytic activity was significantly reduced (30%) relative to that of P450$_{BM3}$, possibly due to a suboptimal electron transfer between the heme and reductase domains.

In the present work, we applied consensus mutagenesis[13] as a strategy to stabilize the reductase domain of P450$_{BM3}$. Following the notion that stability relies on the addition of small contributions of interactions distributed along the sequence,[14] beneficial mutations identified by consensus analysis of a panel of P450$_{BM3}$-related sequences were recombined. Using this approach, we successfully engineered P450$_{BM3}$ variants containing a stabilized reductase domain. The evolved variants exhibit increased half-life and catalytic activity at elevated temperatures as well as a broader temperature range for optimal activity, thus providing a more robust scaffold for engineering studies.

[a]   Dr. V. Guzmán-Luna, Leticia Olvera, and Prof. Dr. G. Saab RIncón
       Departamento de Ingeniería Celular y Biocatálisis, Instituto de
       Biotecnología, Universidad Nacional Autónoma de México,
       Apdo. Postal 510-3, 62250 Cuernavaca, Mor., México
       E-mail: gsaab@ibt.unam.mx
[b]   Hanan Alwaseem and Prof. Dr. R. Fasan
       Department of Chemistry, University of Rochester
       120 Trustee Road, Rochester, NY 14627, United States

       Supporting information for this article is given via a link at the end of
       the document.

Results and Discussion

Consensus analysis and selection of target residues for mutagenesis

A multiple sequence alignment was initially generated (Clustal-W) using 93 non-redundant cytochrome P450 reductase sequences from all orders of life using the sequence of P450$_{BM3}$ reductase domain as template (amino acid residues 480–1049). Detection of a consensus for all positions was not possible however due to the great diversity of sequences included in this set. Accordingly, a cutoff of 38% sequence identity was subsequently applied, resulting in the selection of a smaller subset of 16 homologous sequences, shown in **Figure 1**. Analysis of this dataset enabled the identification of 14 amino acid residues in the P450 BM-3 reductase domain that differ from the consensus residue. For position 915, two consensus amino acids were identified, namely Leu and Ile (compared to Val in P450$_{BM3}$) and therefore both substitutions were considered. As a result of these analyses, the consensus-guided mutations A583R, R612Q, L685I, V760A, A767E, T800S, E803D, E817R, I825L, I825L, Q842R, E853P, S883R, and V915L/I ('consensus' line, **Figure 1**) were selected for the purpose of increasing the stability of P450$_{BM3}$ reductase domain.

Figure 1. Multiple sequence alignment of cytochrome P450 reductases with >38% sequence identity to P450$_{BM3}$ diflavin domain. UniProt entry of each protein is included. Consensus residues are indicated in red in the 'consensus' line. The corresponding target mutations identified via consensus analysis are indicated on top of the sequence list. Numbering of the amino acid residues is relative to the P450$_{BM3}$ sequence.

Mapping of consensus mutations on a model of P450$_{BM3}$ reductase domain

The crystal structure of P450$_{BM3}$ heme domain linked to the FMN-binding domain was previously determined at 2.0 Å resolution.[15] More recently, the crystal structure of the FAD/NADPH-binding domain of this enzyme has been determined in complex with the cofactors at 2.15 Å resolution.[16] To gain insights into the location of the target positions identified by consensus analysis, the corresponding amino acid residues were mapped onto a model of P450$_{BM3}$ reductase domain constructed by combining the aforementioned crystal structures of the FMN- and FAD/NADPH-binding domains, using the rat cytochrome P450 reductase (28% sequence identity) as a template.[17] As shown in **Figure 2A**, most of the selected

positions (11/14) reside within the FAD binding domain, with the remaining three positions residing within the FMN- (2) and NADPH-binding domain (1). Among the residues located within the FAD domain, two pairs of amino acid residues, namely Thr800/Glu803 and Ala767/Glu817, were found to lie in close proximity to each other, suggesting that mutations at these sites may have coevolved. Accordingly, the corresponding consensus-guided mutations (i.e., T800S/E803D and A767E/E817R) were tested in the form of double mutants.
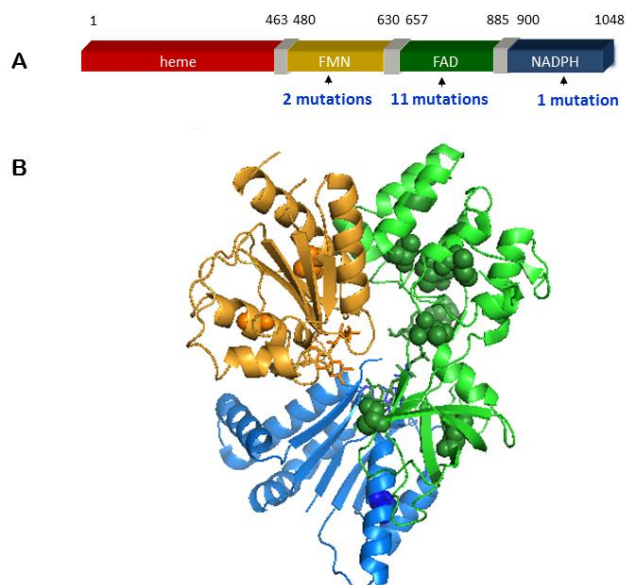
Figure 2. P450$_{BM3}$ sequence and model of its reductase domain. (a) Schematic representation of P450$_{BM3}$ structure highlighting the multi-domain organization of the enzyme. (b) Model of P450$_{BM3}$ reductase domain generated by combining the available structure of P450$_{BM3}$ FMN domain (orange, pdb 1BVY) and FAD/NADPH domains (green/blue; pdb 4DQL) and using the structure of rat P450 reductase as template (pdb 1AMO). The amino acid residues identified by consensus analysis are shown as sphere models and the cofactors as sticks).

Thermal stability of consensus mutagenesis variants

Based on the analyses described above, 13 single mutants and two double mutants of P450$_{BM3}$ reductase domain were constructed and fused to the heme domain of P450$_{BM3}$ variant 4E10.[18] This variant was chosen because it carries two active site mutations (A82L and, A328V) that enable the enzyme with the ability to oxidize non-native substrates such as the chromogenic substrate dimethylether (DME)[6a] and a small-molecule drug, ibuprofen methyl ester[6f], thereby facilitating characterization of the reductase domain variants investigated here. In addition, the two active site mutations in 4E10 have no impact on the stability properties of the enzyme as compared to wild-type P450$_{BM3}$, as determined by measuring half-maximal denaturation temperature (T_{50}) for temperature dependent loss

of heme binding (T$_{50}$ ~ 54°C (**Figure S5**) compared to 55°C for wild-type P450$_{BM3}$.[19]

To assess the stabilizing effects of the reductase domain mutations, the fifteen 4E10-derived variants were screened for retention of DME demethylation activity after a 20-min incubation at 48°C. For convenience, the variants were initially tested using cell lysates and a Purpald-based colorimetric assay[20] to measure the amount of formaldehyde generated upon P450-catalyzed demethylation of DME. As shown in **SI Figure S1**, out of the 14 mutants tested, six showed a significantly higher residual activity than the parental 4E10 enzyme after the incubation period. Based on these results, the beneficial mutations in the corresponding variants (i.e., A583R, L685I, V760A, I825L, E853P, V915L and, V915I) were recombined to generate a second library of twelve P450 variants (called A through P, **Table 1**). This library was screened for residual activity on DME after incubation at 48°C as described above for 30-min, resulting in the identification of nine potentially interesting variants (i.e., A, C, F, G, L, M, N, O, and P). These enzymes were further characterized in purified form by measuring their half-lives at 50°C using the DME/Purpald functional assay (**Figure 3**). Notably, except for variant F, all of the recombination variants exhibited at least a 2-fold increase in half-life compared to 4E10. Among those, variants A, L, M, O, and P were identified as the most thermostable enzymes, showing between 9- and 12-fold longer half-lives compared to the parent 4E10 (Figure 3).

Table 1. Names and amino acid substitutions of P450$_{BM3}$ reductase domain variants investigated in this study.

Variant	Mutations (vs. 4E10)
A	A583R, V760A
B	L685I, V760A
C	A583R, E853P
D	L685I, E853P
E	I825L, E853P
F	V760A, E853P
G	I825L,E853P,V915I
L	A583R, L685I, V760A
M	A583R, L685I, V760A, I825L, E853P, V915I
N	A583R, L685I, V760A, I825L, E853P, V915L
O	A583R, L685I, V760A, I825L, E853P
P	A583R, L685I, V760A, E853P

Determination of optimal temperature

While the half-lives provided in Figure 3 provide a measure of the thermal stability of the enzymes, they do not inform on whether they remain enzymatically active at elevated
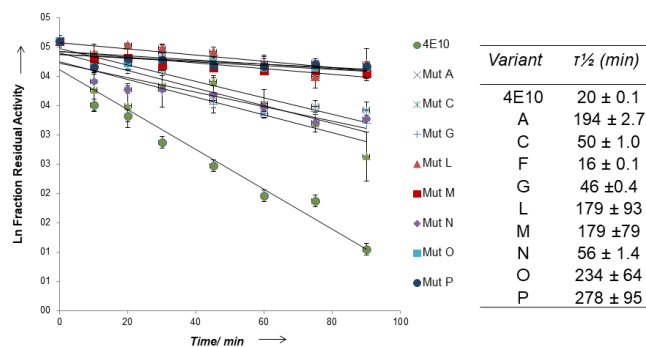
Figure 3. Residual DME oxidation activity and half-lives of P450$_{BM3}$ reductase domain variants at 50 °C. The plot reports the natural logarithm of the enzyme residual activity relative to that of the same protein without thermal treatment. The table shows the estimated half-lives of the enzymes as derived from fitting the experimental data to an exponential decay equation (lines).

temperatures. In order to evaluate this aspect, the P450$_{BM3}$ variants were tested for their oxidation activity on a model non-native substrate, ibuprofen methyl ester (IbuME) (**SI Figure S2**). This compound was better suited for these analyses since, unlike DME, it is not volatile. Initial experiments were carried out by measuring the relative oxidation activity of variants A–P on IbuME over 30 minutes at temperatures ranging from 20°C to 70°C at 10°C intervals. The results are shown in **SI Figure S3** in the form of IbuME oxidation activity relative to that of the same variant at 20°C. Four variants, namely variant C, M, O, and P, showed increased activity than 4E10 at elevated temperature, with product yields being 1.5-3-fold higher at elevated temperatures (≥ 40°C). It is worth mentioning that most of the variants yielded from 20 to 50% more product than 4E10 variant at 20°C. Thus, even though variant A shows a similar profile as the parent enzyme, it produces about 50% more product at 40°C. Interestingly, variant L, which exhibited one of the longest t$_{1/2}$ values (**Figure 3**), did not show significantly improved activity as compared to 4E10 at elevated temperatures. This difference arises from the fact that these experiments effectively measure two different forms of thermal stability, namely the ability to recover monooxygenase activity after thermal exposure and the ability to remain functional as monooxygenases at elevated temperature, respectively. Since the thermostability properties of the latter group of variants are more desirable for conducting reactions at elevated temperatures, these enzymes were selected for further characterization.

To this end, the same experiment was repeated by measuring the IbuME oxidation activity of these variants across a temperature range from 10°C to 60°C at 5°C intervals. The resulting profiles are displayed in **Figure 4A**, in which the enzyme activities are reported as relative to the highest activity measured within the tested temperature range (referred to as "T$_{opt}$ activity"). The parent enzyme 4E10 shows optimal activity between 20 °C and 30 °C and its IbuME oxidation activity rapidly decreases above and below this range. At 40°C, its relative activity is reduced to about 17% of that measured at room temperature. In contrast, variants M, O, and P showed a broader optimal temperature range, which extends to 40°C. In particular, variant M and P exhibit the most interesting activity profile by

retaining 91% and 25% of their T_{opt} activity at 40°C and 45 °C, respectively, compared to 17% and 4%, respectively, for 4E10. Since these enzymatic reactions were performed in the presence of a NADPH cofactor regeneration system containing glucose-6-phosphate dehydrogenase (G6PDH), control experiments were carried out to confirm that this enzyme is stable across the temperature range tested. As shown in **SI Figure S4**, G6PDH shows no significant loss of dehydrogenase activity up to 55°C confirming that the temperature-dependent profiles of **Figure 4A** are solely dependent upon the catalytic activity of the P450s.
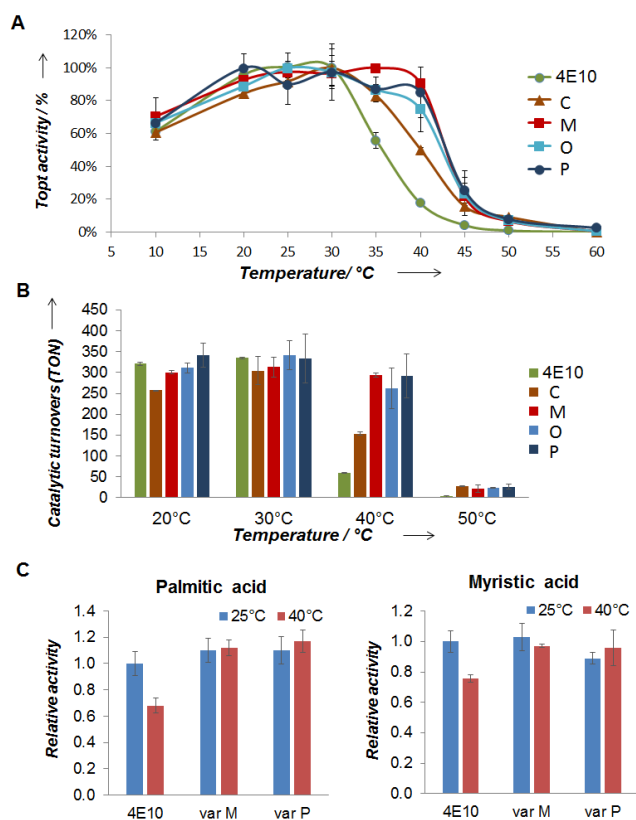
Figure 4. Oxidation activity of P450$_{BM3}$ reductase variants at varying temperature. (A) Temperature dependent profile of ibuprofen methyl ester (IbuME) activity for 4E10 and selected variants, relative to the activity at their optimal temperature. The enzyme activities are reported as relative to the highest activity exhibited by each variant within the tested temperature range. (B) Catalytic turnovers (TON) of 4E10 and selected reductase domain variants for oxidation of ibuprofen methyl ester (IbuME) at different temperatures. (C) Fatty acid oxidation activity for 4E10 and reductase domain variant M and P at room temperature and 40°C. Catalytic activities are normalized to that of the parent P450 (4E10) at room temperature (= 710 TON for palmitic acid and 860 TON for myristic acid).

Catalytic properties of reductase domain variants

To compare the catalytic activity of the most promising reductase domain variants at both room and elevated temperatures, the catalytic turnovers (TON) supported by these enzymes in the oxidation of the drug molecule (IbuME) were

determined at temperatures ranging between 20°C and 50°C. As shown in **Figure 4B**, all of the tested reductase domain variants except variant C, exhibit comparable TON values (~320-330) at room temperature as the parent enzyme 4E10. The activity of the latter drops dramatically at 40°C (58 TON). In contrast, variants M, O, and P still support over 250 TON at this elevated temperature. At 50°C, the catalytic activity of 4E10 is barely detectable (<3 TON), whereas the thermostable variants remain functional, supporting about 20-30 TON. The two most promising variants, M and P, were further characterized for their oxidation activity on the long chain (C_{14}-C_{16}) fatty acid palmitate and myristate, which are preferred substrates for P450$_{BM3}$.[5b] As shown in **Figure 4C**, the fatty acid hydroxylase activity of 4E10 was reduced by up to 40% at elevated temperature (40°C) compared to room temperature. In contrast, variant P and in particular variant M retained parent-like activity on the fatty acid substrates at both room temperature and 40°C. No change in regioselectivity was noted between the reductase variant and the parent protein.

To further examine the effect of the reductase domain mutations on the catalytic properties of the enzymes, product formation rate (PFR) and coupling efficiency in IbuME oxidation were measured for 4E10 and variants M and P (**Table 2**). These experiments revealed that the variants exhibit similar product formation rates (28–35 min^{-1}) and coupling efficiency (9.3–10%) as the parent P450 at room temperature. At elevated temperature (40°C), however, 4E10 showed a reduction in both the product formation rate (-66%) and coupling efficiency (-25%), whereas no effect on either of these parameters was observed for the reductase domain variants upon temperature elevation (Table 2). Taken together, these results showed that the engineered P450$_{BM3}$ variants exhibit improved performance as oxidation catalysts at elevated temperatures. Furthermore, they show that the improvement in thermal stability did not come at the expenses of the catalytic activity or kinetic properties of the P450s at ambient temperature.

Table 2. Product formation rate and coupling efficiency of 4E10 and its variants for the oxidation of ibuprofen methyl ester at 25°C and 40°C. Coupling efficiency is given by the ratio between the product formation rate and the NADPH oxidation rate in the presence of the substrate.

Variant	Temperature (°C)	NADPH ox rate (min^{-1})	PFR (min^{-1})	Coupling Efficiency
4E10	25	290 ± 14	28 ± 3	10%
	40	130 ± 10	10 ± 3	7%
M	25	300 ± 14	31 ± 2	11%
	40	340 ± 12	35 ± 4	10%
P	25	380 ± 16	35 ± 4	9%
	40	330 ± 13	34 ± 7	10%

Analysis of Electron Transfer Properties

In P450$_{BM3}$, the electrons required to support the catalytic cycle flow from the soluble NADPH cofactor to the protein bound

flavin and heme prosthetic groups in the order: NADPH→ FAD →FMN→heme.[21] In the presence of NADPH, P450$_{BM3}$ can reduce a variety of artificial electron acceptors such as cytochrome *c* and potassium ferricyanide.[22]. It was previously established that cytochrome *c* reduction involves FMN as the electron donor, whereas potassium ferricyanide accepts electrons directly from the FAD.[21-22, 23] The rates at which these artificial electron acceptors are reduced by the reductase domain variants can therefore be used to evaluate the functionality of the FMN and FAD domain of these enzymes during the electron transfer process. Accordingly, the rates of cytochrome *c* and potassium ferricyanide reduction were measured for both 4E10 and the stabilized variants M and P variants at both ambient and elevated temperature (40 °C) (**Table 3**). At room temperature, a 2-fold increase in ferricyanide reductase activity was observed for both variant M and P, relative to 4E10. An increase in temperature from 25°C to 40°C results in a 90% decrease in reductase activity for the parent enzyme (**Table 3**). In contrast, variants M and P retain 90% and 67%, respectively, of the ferricyanide reduction activity measured at room temperature. Similar to the ferricyanide reduction, variants M and P showed higher cytochrome *c* reduction rates (+45% and +39%, respectively) relative to 4E10. At 40 °C, the parent enzyme exhibits negligible cytochrome *c* reductase activity (2 min^{-1}), corresponding to a >99.9% decrease in reduction rate compared to ambient temperature (4,300 min^{-1}). Variant P also shows a noticeable drop in cytochrome *c* reductase activity but, unlike for 4E10, the diminished electron transfer properties of the FMN domain in this variant do not translate in reduced monooxygenase activity, as evidenced by the data provided in Table 2. Variant M, on the other hand, displays remarkable tolerance to elevated temperatures maintaining approximately 75% of the cytochrome *c* reduction activity measured at room temperature. Based on these and previous data, variant M emerged as the most interesting variant in terms of catalytic activity and thermal stability properties and it was therefore selected for further biophysical characterization.

Table 3. Initial rates for reduction of artificial electron acceptors for 4E10 and its reductase domain variants at different temperatures.

Variant	Temperature (°C)	Ferricyanide reduction rate (min^{-1})	Cyt *c* reduction rate (min^{-1})
4E10	25	4,300 ± 210	4,200 ± 355
	40	480 ± 105	2 ± 1
M	25	8,100 ± 370	6,100 ± 115
	40	7,300 ± 205	3,900 ± 535
P	25	8,200 ± 180	5,900 ± 150
	40	5,500 ± 980	540 ± 120

Analysis of structural changes and thermal stability by circular dichroism (CD)

Far-UV (190–260 nm) CD spectra provide information about the secondary structure content of a protein, whereas the

near-UV and visible ranges of these spectra (260–610 nm) are informative of changes in its tertiary structure. The far-UV CD spectra of 4E10 and variant M show two negative bands of similar magnitude at 222 and 208 nm and a positive band at ~190 nm, characteristic of a protein with a significant content of α-helices (**Figure 5A**). Both spectra are practically undistinguishable, indicating that there was not perturbation in secondary structure by the six mutations accumulated in the engineered P450. The near UV and visible CD spectra of these enzymes also exhibited marked similarities (**Figure 5B**). The spectrum of variant M exhibits a slightly more negative signal around 280–286 nm, which arise mainly from aromatic amino acid chains and around 360-560 nm, which derives from the cofactors (**Figure 5B**). Overall, based on the close similarity between the CD spectra of the two proteins, it can be derived that the mutations carried by the stabilized variant M have no major effects on the global secondary and tertiary structure of the protein.

Thermal denaturation experiments were then performed to examine the effect of the mutations on the relative stability of these P450s. Temperature-induced changes in secondary and tertiary interactions were analyzed by monitoring the CD signal at 220 nm (**Figure 5C**) and 285 nm (**Figure 5D**), respectively. The thermal unfolding curves of the P450$_{BM3}$ variants as monitored at both wavelengths showed two major transitions and the data were thus fit to double-sigmoid functions. Differential Scanning Calorimetric (DSC) analysis of P450$_{BM3}$ has previously shown that the heme domain is more thermostable than the reductase domain.[11] Accordingly, the biphasic transitions of **Figure 5C** and **5D** can be assigned to the unfolding of the reductase domain (lower temperature transition) and of the heme domain (higher temperature transition). When
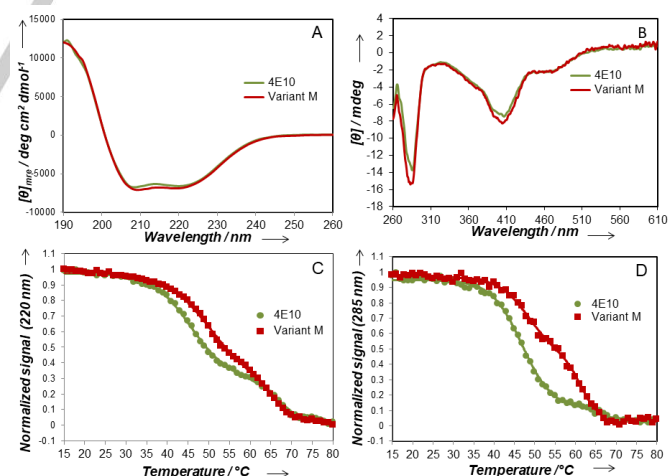
Figure 5. Circular dichroism studies. (A) Far-UV and (B) visible CD spectra of 4E10 (green), and variant M (red). All spectra were recorded at 25°C. (C-D) Temperature-induced conformational transitions of the P450$_{BM3}$ variants: 4E10 (green circles), and Mut M (red squares), monitored at CD wavelengths of 220 nm (C) and 285 nm (D). Continuous line of Panels C-D fits to double-sigmoid function. Data represent the average of three independent experiments. Error bars were removed for clarity.

For internal use, please do not delete. Submitted_Manuscript

monitored at 220 nm, thermal unfolding of 4E10 shows an apparent melting temperature (T_m^{app}) of 45.6°C for the reductase domain and of 67.1°C for the heme domain (**Table 4**). These values are in general agreement with the reported T_m values of 48°C (reductase) and 63°C (heme) as measured with P450$_{BM3}$ by DSC.[11]. Notably, the thermal unfolding curve of variant M shows a shift of the low-temperature transition to a higher temperature range (**Figure 5D**). In this case, the calculated T_m values for the reductase domain of variant M is 50.5°C (**Table 4**), thereby indicating a significant increase (ΔT_m: +4.9°C) in the thermostability of this domain compared to the parent P450. A similar result (ΔT_m: +2.9°C) was obtained by monitoring unfolding at 285 nm (**Table 4**). At this wavelength, a reduction of the T_m for the heme domain was noticed, suggesting that while the stability of secondary structures of the heme domain is unaffected by the reductase domain mutations, tertiary structure interactions are somewhat affected perhaps due to domain-domain interactions. In any case, the T_m of the heme remains higher than that of the reductase domain. Furthermore, the thermal stability of the heme domains in M and the parent P450 were found to be essentially identical based on T$_{50}$ measurements (T$_{50}$ = 54.7°C vs. 53.7°C, respectively; **Figure S5**).

The ability of the P450s to tolerate and refold after exposure to elevated temperatures was also examined. Both variants were determined to unfold irreversibly when heated to 80°C. At 55°C, which corresponds to the plateau observed between the two thermal transitions (**Figure 5C**), variant M maintains a higher degree of folded structure compared to 4E10, as revealed by comparison of the near-UV and visible regions of their respective CD spectra (**Figure 6C and 6D**, dashed line). After exposure to 55°C, variant M is able to refold completely, giving a CD spectrum that is superimposable to that of the protein prior to thermal incubation (**Figure 6B and 6D**, dotted line). In contrast, tertiary structure interactions corresponding to reductase domain are not completely recovered in 4E10 **(Figure 6C)**. Taken together, the results described above support the beneficial effects of the mutations toward increasing the thermostability of the reductase domain of variant M and its tolerance against thermal inactivation.

Table 4. Apparent melting temperatures for the heme and reductase domain of 4E10 and variant M as determined by thermal denaturation analyses via CD. The temperature-induced change in CD signal was monitored at both 220 and 285 nm.

Variant	T_m^{app} (220 nm)		T_m^{app} (285 nm)	
	Heme domain	Reductase domain	Heme domain	Reductase domain
4E10	67 ± 1	46 ± 1	67 ± 1	47 ± 1
M	66 ± 1	51 ± 1	61 ± 1	50 ± 1

Structure content of the reductase domain

The two most stable 4E10 derivatives, variants M and P, share a total of four mutations, with variant M containing two additional mutations at position 825 and 915 (**Table 1**). Most of these amino acid substitutions are conservative in nature (L685I, V760A, I825L, and V915I), whereas A583R and E853P are not. In an effort to rationalize their stabilizing effect, these mutations were modeled in the structure of the P450$_{BM3}$ reductase domain (**Figure 7A**). Ala583 is located in an α-helical region of the FMN-binding domain in proximity to the FMN cofactor (**Figure 7B**). *In silico* analysis of the A583R mutation suggests that introduction of an arginine residue at this position could enable formation of polar interactions (~3 Å distance) between the guanidinium group and the nearby Glu602 and Tyr578 residues, which are part of the FMN binding site (**Figure 7B**). Mutation E853P, on the other hand, affects a residue (Glu853) that is part of the
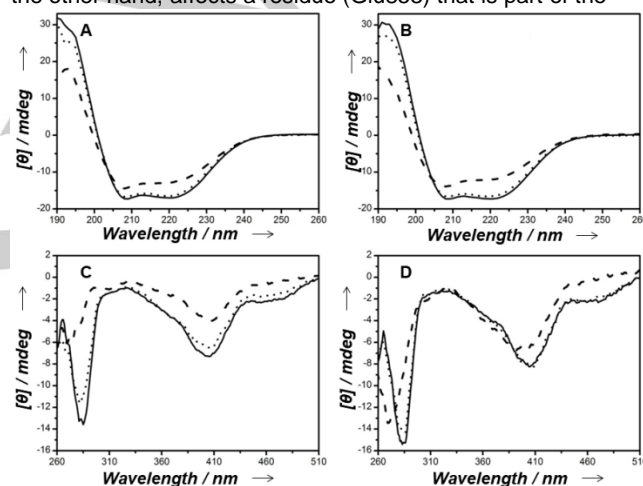
Figure 6. Far UV CD spectra of stable species of 4E10 (A) and variant M (B). Near and visible CD spectra of stable species of 4E10 (C) and Mut M (D). In Panels A-D solid lines are the native species, dashed lines are species at 55°C and dotted lines are the refolded species.

FAD-binding site.[16] Glu853 is located at the C-terminus of a β-hairpin motif (**Figure 7C**). Pro residues are rarely found in β-strands but , when present, they have a high preference for both cap positions of β-strands[24], which could justify the stabilizing effect of this mutation at this site. The combination of these two mutations alone resulted in a 2-fold longer half-time at 50°C (variant C; **Figure 3**), suggesting that these mutations contribute to only part of the increased stability exhibited by variant M and P.

Modeling of the conservative substitutions L685I, I825L, and V915I suggest that these mutations could contribute to a better packing of the hydrophobic core within the FAD domain. Specifically, the side chain of Ile685 lies within van der Waals contact distance with the aliphatic side chains of the nearby residues Ala669 and Leu869 (**Figure 7E**). Similarly, I825L mutation could increase the packing of the lateral chain with residues 752-755 in a loop that precedes residue Gln757, which is part of the FAD-binding site (**Figure 7F**). As shown in **Figure**

7D, the introduction of isoleucine at position 915 forms a hydrophobic cluster with the side chains of Ile915, Leu950, and Ile959 from α-helices 10 and 11. Therefore, mutation V915I could strengthen the hydrophobic interactions between these α-helices. The beneficial role of this mutation is also apparent from the 3-fold longer half-life (50°C) of variant M compared to variant N (**Figure 3**), which differ from each other by the residue (Ile vs. Leu, respectively) at position 915 (**Table 1**). Finally, the stabilizing effect of mutation V760A may stem from an increase in the conformational flexibility of a linker region within the FAD domain (**Figure 7G**). Position 759 is occupied by a Pro, which is a conformationally constrained residue, and substitution of the β-branched alkyl chain with a methyl group as a result of the V760A substitution is expected to increase the flexibility of the protein backbone spanning these residues.
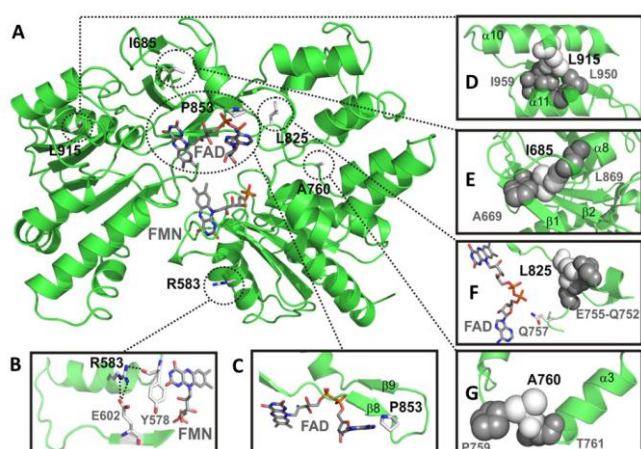
Figure 7. Structure of P450_BM3 reductase domain, in which the mutations of the stabilized variant M and P have been modeled. The FAD/FMN domains are shown as ribbon model (green) with the flavin cofactors being highlighted as stick models (grey). The boxes provide close-up views for the modeled residues: (b) Arg583, (c) Pro853, (d) Leu915, (e) Ile685, (f) Leu825, and (g) Ala760.

Conclusions

Directed evolution has proven effective in increasing protein stability,[25] but this process typically involves several rounds of mutagenesis and screening to achieve step-wise improvements in thermostability. This process can be accelerated by the use of phylogenetic information, since it provides a means to confine sequence space to be explored, reducing screening efforts.[26] In this study, we showed how consensus analysis allowed for the identification of beneficial mutations to increase the stability of the reductase domain of a multidomain P450. The combination of multiple consensus mutations has resulted in two P450_BM3 variants with enhanced robustness toward thermal inactivation ($t_{1/2}$) as well as improved catalytic performance at elevated temperature. Importantly, the stabilization process did not come at the expenses of the catalytic activity of the enzyme at ambient

temperature. The thermostabilization of the reductase domain was corroborated by thermal denaturation experiments (CD) and is likely to stem from the combined stabilizing effect of multiple mutations within the FAD and FMN domain of the enzyme. The thermostable P450_BM3 variants described here are expected to facilitate efforts toward engineering this valuable P450 enzyme for a broad range of synthetic and biotechnological applications.

Experimental Section

Materials and Reagents. Enzymes for DNA manipulations were obtained from New England Biolabs (Beverly, MA) and Stratagene (La Jolla, CA). Synthetic oligo-nucleotides were purchased from Operon (Huntsville, Alabama). DNA purification kits were from Zymo Research (Orange, CA) and Qiagen (Valencia, CA). Other reagents and chemicals were from Fisher Scientific (Pittsburgh, PA), Becton Dickinson (Franklin Lake, NJ), and Sigma Chemical Co. (St. Louis, MO). DH5αF´ *Escherichia coli* strain was transformed with all constructs. The P450 BM-3 gene was cloned in the β-D-thiogalactopyranoside (IPTG)-inducible pCWori+ vector.[27] P450_BM3 variant 4E10 was previously described[6a].

Consensus sequence analysis. Identification of close orthologous was obtained by running a blastp search[28] against the KEGG genome database using the sequence corresponding to the reductase domain of P450_BM3 (residues 480–1049) as query. A comprehensive sequence alignment was carried out using CLUSTALW[29] with a cutoff of 38% sequence identity.

Molecular modelling. The structural model for P450_BM3 reductase domain was assembled with Pymol (http://sourceforge.pymol.org) using the available crystal structure of the FAD/NADPH (PDB: 4DQL, chain A)[16] and FMN (PDB: 1BVY, chain F)[15] domains of this enzyme and the crystal structure of rat cyt P450 reductase as template (PDB: 1AMO)[17]. Yasara software[30] was used to optimize geometries, release local constraints, correct possible inappropriate contacts, and for energy minimization of the model. The mutations shown in **Figure 7** were modeled using PyMOL.

Site-directed mutagenesis: The single- and multiple-site variants were constructed using the PCR driven overlapping extension protocol.[31] The final products containing the reductase domain gene were cloned into the *Sac* I/*EcoR* I cassette in pCWori vector containing the P450_BM3 variant 4E10. This variant contains a SacI restriction site between the heme and the reductase domain. The multiple mutants were constructed by assembling the PCR products obtained with the different mutagenic oligo-nucleotides. The oligonucleotide sequences for the mutations are shown in **SI Table S1**. The ligated products were transformed into DH5α *E. coli* competent cells and confirmed by DNA sequencing.

Thermal stability assay (DME). Cultures expressing the P450 variants were grown in terrific broth (TB) in 96 deep-well plates (four replicates). After four hours, protein expression was induced by the addition of 0.25 mM IPTG and cell growth continued at 30°C overnight. The plates were centrifuged, and cell pellets were frozen at -20°C. For analysis, the cells were lysed in 100 mM phosphate buffer, 10 mM MgCl₂, pH 8.0, containing lysozyme (0.5–1 mg/mL) and DNase I (10 units/mL). Clarified cell lysates were transferred to 96-well microplates for activity measurements at room temperature. Lysates were also transferred to 96-well PCR plates (GeneMate) and heated at 48 °C for 20 min in a water bath, rapidly cooled to 4°C, and then brought to room temperature. The oxidation activity of the P450 variants prior to and after heat treatment

was assayed using dimethyl ether as described previously.[6a] Briefly, 120 µL of phosphate buffer 0.1 M, pH 8, saturated with dimethyl ether were added to 30 µL of cell lysate containing the P450 enzyme. After 2 min of incubation at room temperature, 50 µL of 1 mM NADPH were added. After 15 min, 50 µL of purpald (168 mM in 2 M NaOH) were added to the reaction mixture. The purple product was quantified by measuring the absorbance at 550 nm using a Spectramax Plus microtiter plate reader. The half-life ($t_{1/2}$) values were determined using purified enzymes (70 µM) incubated at 50°C in triplicate. Samples were removed at time intervals, quenched by placing into an ice bath, brought to room temperature, and assayed for residual DME activity using the assay described above.

T_{50} analysis. To determine heme domain stability, 50 µL of a 40-60 µM protein solution (50 mM potassium phosphate buffer, pH 8.0) were incubated for 10 minutes at varying temperature between 20°C and 90°C. After incubation, the solution was cooled on ice, diluted in potassium phosphate buffer and centrifuged (14,000 rpm) for ten minutes. The supernatant was transferred to a cuvette and the amount of correctly folded P450 (λ_{max} = 450 nm) was determined via CO-difference spectrum using $\epsilon_{450-490}$ = 91 mM^{-1} cm^{-1} and sodium dithionite as the reductant Half-maximal denaturation temperatures (T_{50}) were calculated from the concentration of active protein vs. temperature plots by fitting the data to a four-parameter sigmoidal equation in GraphPad Prism (**Figure S5**). The reported mean values and standard errors were derived from experiments performed in duplicate.

Protein expression and purification. After expression, the cell pellet was resuspended with Tris-HCl (15 mL, 25 m M, pH 8.0) and lysed by sonication. The lysate was centrifuged at 23,300 g for 1 hour and further cleared through a 0.45 µM filter. The filtrate was loaded on a DEAE anion exchange column previously equilibrated with the same buffer and washed with six column volumes (cv) of 25 mM Tris pH 8.0, washed with 10 volumes of 25 mM Tris-HCl, 133 mM NaCl, pH 8.0 and finally eluted with 25 mM Tris-HCl, 250 mM NaCl, pH 8.0 buffer. The protein was concentrated and dialyzed by ultrafiltration with 100 mM phosphate buffer, pH 8.0. The concentrated protein was stored at -70°C. P450 concentration was calculated from the CO-difference spectrum using $\epsilon_{450-490}$ = 91 mM^{-1} cm^{-1}.[32] For biophysical characterization, BL21 Gold *E. coli* cells were transformed with the pCWori plasmid encoding for the P450. Transformed cells were grown in terrific broth containing 150 mg ampicillin/L at 37°C until OD$_{600}$ reached 0.6. Protein expression was induced by addition of IPTG (1 mM) and incubated for another 12 hours at 30°C. After harvesting the cells at 10,400 g for 20 min, the pellet was resuspended in a 30 mM Tris buffer containing 0.1 mM EDTA, 0.5 mM DTT, 0.1 mM PMSF, pH 7.4 (buffer A) and sonicated. The cell lysate was clarified by centrifugation (12,100 g, 30 min) and filtration through a 0.22-µm membrane and then loaded on a MonoQ HR 16/10 column (GE Healthcare). The column was washed with two column volumes of buffer B (30 mM Tris, 250 mM NaCl, 0.1mM EDTA, 0.5 mM DTT, 0.1 mM PMSF buffer at pH 7.4) and the protein was eluted with 2.5 volumes gradient of NaCl from 250 to 400 mM. Pure fractions (>95% purity), as assessed by sodium dodecyl sulfate/polyacrylamide gel electrophoresis (SDS PAGE), were consolidated and dialyzed against 10 mM phosphate buffer (pH 7.4) containing 0.5 mM DTT. The protein concentration was determined by the Bradford assay (Bio-Rad).

Temperature dependent oxidation activity profiles. 4E10-catalyzed oxidation of ibuprofen methyl ester (IbuME) produces two hydroxylation products in approximately a 7:2 ratio. From titration experiments (**SI Figure S2**), a substrate concentration of 1 mM was chosen as optimal for the IbuME activity measurements. IbuME oxidation activity was measured by dissolving IbuME at 1 mM (from a 100 mM ethanol stock) in 900 µL phosphate buffer pH 8.0. Enzyme was added at final

concentration of 750 nM. The mixture was pre-incubated at the desired temperature for two minutes in a thermoblock (700 rpm). After pre-incubation, the reaction was started by adding 100 µL of a 10x cofactor regeneration solution (4 mM NADP$^+$, 20 mM glucose-6-phosphate, 10 U/mL glucose-6-phosphate dehydrogenase). The reaction was incubated at the desired temperature for 30 min (700 rpm) and stopped by the addition of 50 µL 2 N HCl. The reaction mixture was added with internal standard (500 µM guaiacol), extracted with 200 µL dichloromethane, and analysed by gas chromatography. Using this protocol, parent 4E10 and all the variants were tested in duplicate for activity at the indicated temperature between 20 and 70°C. Relative activities were obtained by normalization to the IbuME oxidation activity of the enzyme measured at 20°C. Catalytic turnovers (TON) for IbuME oxidation (30 min) were measured based on the total GC peak area for the hydroxylated IbuME products using calibration curves of authentic standards.[6f] Control experiments were carried out to confirm that the measured P450 oxidation activity at elevated temperature is not limited by the stability of the G6PDH enzyme used in the NADPH cofactor regeneration system (**SI Figures S3**).

Product formation rates and coupling efficiency for IbuME oxidation. Initial product formation rates were measured using 1 mL-scale reactions containing 0.5 µM P450, 0.5 mM IbuME, and 2 mM NADPH in 50 mM potassium phosphate buffer (pH 8.0). The reaction mixture was pre-incubated at the desired temperature for ten minutes prior to addition of NADPH. After 30 seconds, the reaction was quenched by the addition of 50 µL 2 N HCl. After addition of the internal standard (500 µM guaiacol), the mixtures were extracted with 300 µL dichloromethane and analyzed by gas chromatography. The coupling efficiency was determined as the ratio between rates of product formation and NADPH consumption in the presence of the substrate. The NADPH consumption rate was monitored at 340 nm (ϵ = 6.22 mM^{-1} cm^{-1}) under the same conditions as the product formation rate experiments. The cuvette samples were also pre-incubated at the desired temperature for ten minutes prior to addition of NADPH.

Fatty acid oxidation activity. The oxidation activity on palmitate and myristate was measured through 1 mL-reactions containing 1 mM substrate and 1 µM P450 enzyme in 50 mM phosphate buffer (pH 8.0). The mixture was pre-incubated at the desired temperature for 15 minutes in a temperature-controlled incubator and started by adding 10 µL of a 1 M NADPH stock solution. The reaction was incubated at the desired temperature for four hours and quenched by addition of 50 µL HCl 2 N. Internal standard (guaiacol, 500 uM) was added to the reaction mixture and the solution was extracted with 200 µL dichloromethane and dried over sodium sulphate. The fatty acids were then derivatized by addition of 20 µL MSTFA (N-methyl-N-(trimethylsilyl)-trifluoroacetamide) at 50°C for 3 hours, followed by GC analysis.

Determination of ferricyanide and cytochrome c reductase activity: The assays were conducted at a 1-mL scale in 50 mM potassium phosphate buffer (pH 8.0). Ferricyanide reductase activity was monitored by measuring the decrease in absorbance at 420 nm (ϵ = 1.02 mM^{-1} cm^{-1}) in a cuvette containing 33 nM P450, 100 µM NADPH, and 500 µM K$_3$Fe(CN)$_6$. NADPH was added after incubation of the samples for ten minutes at the desired temperature. Cytochrome *c* reductase activity was assayed by monitoring the increase in absorbance at 550 nM (ϵ = 21.1 mM^{-1} cm^{-1}). The samples contained: 33 nM P450, 100 µM NADPH, and 60 µM cytochrome *c* (from equine heart). The cuvettes were pre-incubated at the desired temperature for ten minutes prior to addition of NADPH.

CD Spectroscopy: CD spectra were recorded using a Jasco J-715 CD spectropolarimeter (JASCO Analytical Instruments) equipped with a

Peltier temperature-controlled cell holder (PTC-4235, JASCO). The far-UV spectra (190–260 nm) were recorded using 1.7 µM enzyme in a 0.1 cm path length quartz cell Four spectra were averaged to reduce noise. Each spectrum was acquired every 1 nm with eight seconds average time per point and 1 nm band pass. The temperature dependence of the secondary structure was studied by monitoring the CD signal at 220 nm. The CD spectra in the near-UV and visible region (260–610 nm) were recorded using 10.7 µM of the enzyme in a quartz cuvette of 1 cm path length. The temperature dependence of the CD signal for the tertiary interactions and the structure of the FAD, FMN, and heme-binding domains were monitored at 285, 388, and 475 nm. Experiments were performed with at least three independent freshly prepared samples in 10 mM phosphate buffer (pH 7.4). The temperature ranges monitored were 15–80 °C and 15–55 °C. The temperature scans were performed with a data pitch of 1 °C at a rate of 1°C/min. Refolding transitions were performed five seconds after the unfolding transitions had been completed.

Data analysis: The thermal unfolding data, monitored at 220 and 285 nm, were fit to a double-sigmoid function. Fits to sigmoid functions were used to determine the apparent T_m (T_m^{app}) and the cooperativity (c) for the unfolding transitions, as follows:

$$y_{obs} = y_0 + A\left[\frac{f_r}{1+e^{(T-Tm_r)/c_r}} + \frac{1-f_r}{1+e^{(T-Tm_{cyt})/c_{cyt}}}\right] \qquad \text{Ec. 1}$$

where y_{obs} is the CD normalized signal at the particular wavelength; y_0 is the signal for the unfolded state; A is the signal for the native state, f_r is the signal for the I state; Tm_r and Tm_{cyt} are the apparent Tm values for the unfolding of N and I, respectively; c_r and c_{cyt} are the unfolding cooperativity indexes of N and I, respectively.

Acknowledgements

Keywords: Cytochrome P450 • Consensus mutagenesis • Enzyme thermostabilization • P450 BM-3 • CYP102A1

References

[1]   a) I. G. Denisov, T. M. Makris, S. G. Sligar, I. Schlichting, *Chem. Rev.* **2005**, *105*, 2253-2277; b) P. R. O. de Montellano, *Chem. Rev.* **2010**, *110*, 932-948; c) F. P. Guengerich, A. W. Munro, *J. Biol. Chem.* **2013**, *288*, 17065-17073.

[2]   a) R. Fasan, *ACS Catal.* **2012**, *2*, 647-666; b) G. Grogan, *Curr. Opin. Chem. Biol.* **2011**, *15*, 241-248; c) H. M. Girvan, A. W. Munro, *Curr. Opin. Chem. Biol.* **2016**, *31*, 136-145.

[3]   a) L. O. Narhi, A. J. Fulco, *J. Biol. Chem.* **1986**, *261*, 7160-7169; b) R. T. Ruettinger, L. P. Wen, A. J. Fulco, *J. Biol. Chem.* **1989**, *264*, 10987-10995.

[4]   A. J. Warman, O. Roitel, R. Neeli, H. M. Girvan, H. E. Seward, S. A. Murray, K. J. McLean, M. G. Joyce, H. Toogood, R. A. Holt, D. Leys, N. S. Scrutton, A. W. Munro, *Biochem. Soc. T.* **2005**, *33*, 747-753.

[5]   a) S. T. Jung, R. Lauchli, F. H. Arnold, *Curr. Opin. Biotechnol.* **2011**, *22*, 809-817; b) C. J. C. Whitehouse, S. G. Bell, L. L. Wong, *Chem. Soc. Rev.* **2012**, *41*, 1218-1260.

[6]   a) M. W. Peters, P. Meinhold, A. Glieder, F. H. Arnold, *J. Am. Chem. Soc.* **2003**, *125*, 13442-13450; b) D. Appel, S. Lutz-Wahl, P. Fischer, U. Schwaneberg, R. D. Schmid, *J. Biotechnol.* **2001**, *88*, 167-171; c) J. B. Behrendorff, W. Huang, E. M. Gillam, *Biochem. J.* **2015**, *467*, 1-15; d) D. F. Munzer, P. Meinhold, M. W. Peters, S. Feichtenhofer, H. Griengl, F. H. Arnold, A. Glieder, A. de Raadt, *Chem. Commun. (Camb.)* **2005**, 2597-2599; e) W. T. Sulistyaningdyah, J. Ogawa, Q. S. Li, C. Maeda, Y. Yano, R. D. Schmid, S. Shimizu, *Appl. Microbiol. Biotechnol.* **2005**, *67*, 556-562; f) A. Rentmeister, F. H. Arnold, R. Fasan, *Nat. Chem. Biol.* **2009**, *5*, 26-28; g) M. Dietrich, T. A. Do, R. D. Schmid, J. Pleiss, V. B. Urlacher, *J. Biotechnol.* **2009**, *139*, 115-117; h) C. J. Whitehouse, S. G. Bell, W. Yang, J. A. Yorke, C. F. Blanford, A. J. Strong, E. J. Morse, M. Bartlam, Z. Rao, L. L. Wong, *Chembiochem* **2009**, *10*, 1654-1656; i) E. Weber, A. Seifert, M. Antonovici, C. Geinitz, J. Pleiss, V. B. Urlacher, *Chem. Commun. (Camb.)* **2011**, *47*, 944-946; j) R. Agudo, G. D. Roiban, M. T. Reetz, *Chembiochem : a European journal of chemical biology* **2012**, *13*, 1465-1473; k) A. T. Li, A. Ilie, Z. T. Sun, R. Lonsdale, J. H. Xu, M. T. Reetz, *Angew. Chem. Int. Ed.* **2016**, *55*, 12026-12029.

[7]   a) M. C. Damsten, B. M. van Vugt-Lussenburg, T. Zeldenthuis, J. S. de Vlieger, J. N. Commandeur, N. P. Vermeulen, *Chem. Biol. Interact.* **2008**, *171*, 96-107; b) A. M. Sawayama, M. M. Chen, P. Kulanthaivel, M. S. Kuo, H. Hemmerle, F. H. Arnold, *Chemistry (Weinheim an der Bergstrasse, Germany)* **2009**, *15*, 11723-11729; c) A. Rentmeister, T. R. Brown, C. D. Snow, M. N. Carbone, F. H. Arnold, *Chemcatchem* **2011**, *3*, 1065-1071.

[8]   K. Zhang, S. El Damaty, R. Fasan, *J Am Chem Soc* **2011**, *133*, 3242-3245.

[9]   a) P. Meinhold, M. W. Peters, M. M. Chen, K. Takahashi, F. H. Arnold, *Chembiochem* **2005**, *6*, 1765-1768; b) R. Fasan, N. C. Crook, M. W. Peters, P. Meinhold, T. Buelter, M. Landwehr, P. C. Cirino, F. H. Arnold, *Biotechnol. Bioeng.* **2011**, *108*, 500-510.

[10]   a) O. Salazar, P. C. Cirino, F. H. Arnold, *Chembiochem* **2003**, *4*, 891-893; b) Y. G. Li, D. A. Drummond, A. M. Sawayama, C. D. Snow, J. D. Bloom, F. H. Arnold, *Nature Biotechnol.* **2007**, *25*, 1488-1488.

[11]   A. W. Munro, J. G. Lindsay, J. R. Coggins, S. M. Kelly, N. C. Price, *Biochim. Biophys. Acta* **1996**, *1296*, 127-137.

[12]   S. Eiben, H. Bartelmas, V. B. Urlacher, *Appl. Microbiol. Biotechnol.* **2007**, *75*, 1055-1061.

[13]   a) M. Lehmann, L. Pasamontes, S. F. Lassen, M. Wyss, *Biochim. Biophys. Acta* **2000**, *1543*, 408-415; b) M. Lehmann, M. Wyss, *Curr. Opin. Biotechnol.* **2001**, *12*, 371-375.

[14]   a) M. H. Hecht, J. M. Sturtevant, R. T. Sauer, *Proteins* **1986**, *1*, 43-46; b) M. Matsumura, S. Yasumura, S. Aiba, *Nature* **1986**, *323*, 356-358; c) M. W. Pantoliano, M. Whitlow, J. F. Wood, S. W. Dodd, K. D. Hardman, M. L. Rollence, P. N. Bryan, *Biochemistry* **1989**, *28*, 7205-7213.

[15]   I. F. Sevrioukova, H. Li, H. Zhang, J. A. Peterson, T. L. Poulos, *Proc. Natl. Acad. Sci. U. S. A.* **1999**, *96*, 1863-1868.

[16]   M. G. Joyce, I. S. Ekanem, O. Roitel, A. J. Dunford, R. Neeli, H. M. Girvan, G. J. Baker, R. A. Curtis, A. W. Munro, D. Leys, *FEBS J.* **2012**, *279*, 1694-1706.

[17]   M. Wang, D. L. Roberts, R. Paschke, T. M. Shea, B. S. Masters, J. J. Kim, *Proc. Natl. Acad. Sci. U. S. A.* **1997**, *94*, 8411-8416.

[18]   M. M. Y. Chen, C. D. Snow, C. L. Vizcarra, S. L. Mayo, F. H. Arnold, *Protein Eng. Des. Sel.* **2012**, *25*, 171-178.

[19]   R. Fasan, M. M. Chen, N. C. Crook, F. H. Arnold, *Angew Chem Int Ed Engl* **2007**, *46*, 8414-8418.

[20]   H. B. Hopps, *Aldrichimica Acta* **2000**, *33*, 28-30.

[21]   J. L. Vermilion, D. P. Ballou, V. Massey, M. J. Coon, *J. Biol. Chem.* **1981**, *256*, 266-277.

[22]   a) M. L. Klein, A. J. Fulco, *J. Biol. Chem.* **1993**, *268*, 7553-7561; b) M. B. Murataliev, R. Feyereisen, *Biochemistry* **1996**, *35*, 15029-15037.

[23]   G. P. Kurzban, H. W. Strobel, *J. Biol. Chem.* **1986**, *261*, 7824-7830.

For internal use, please do not delete. Submitted_Manuscript

[24]   N. Bhattacharjee, P. Biswas, *BMC Struct. Biol.* **2010**, *10*, 29.
[25]   a) J. L. Carter, M. Bekhouche, A. Noiriel, L. J. Blum, B. Doumeche,
         Chembiochem **2014**, *15*, 2710-2718; b) L. Giver, A. Gershenson, P.
         O. Freskgard, F. H. Arnold, *Proc. Natl. Acad. Sci. U. S. A.* **1998**, *95*,
         12809-12813; c) M. Z. Kamal, S. Ahmad, T. R. Molugu, A.
         Vijayalakshmi, M. V. Deshmukh, R. Sankaranarayanan, N. M. Rao,
         J. Mol. Biol. **2011**, *413*, 726-741; d) H. J. Wijma, R. J. Floor, P. A.
         Jekel, D. Baker, S. J. Marrink, D. B. Janssen, *Protein Eng. Des.
         Sel.* **2014**, *27*, 49-58; e) I. Wu, F. H. Arnold, *Biotechnol. Bioeng.*
         2013, *110*, 1874-1883; f) N. Zhang, W. C. Suen, W. Windsor, L.
         Xiao, V. Madison, A. Zaks, *Protein Eng.* **2003**, *16*, 599-605; g) H.
         Zhao, F. H. Arnold, *Protein Eng.* **1999**, *12*, 47-53.
[26]   a) N. Amin, A. D. Liu, S. Ramer, W. Aehle, D. Meijer, M. Metin, S.
         Wong, P. Gualfetti, V. Schellenberger, *Protein Eng. Des. Sel.* **2004**,
         17, 787-793; b) Y. Ito, A. Ikeuchi, C. Imamura, *Protein Eng. Des.
         Sel.* **2013**, *26*, 73-79.
[27]   H. J. Barnes, M. P. Arlotto, M. R. Waterman, *Proc. Natl. Acad. Sci.
         U. S. A.* **1991**, *88*, 5597-5601.
[28]   S. F. Altschul, T. L. Madden, A. A. Schaffer, J. Zhang, Z. Zhang, W.
         Miller, D. J. Lipman, *Nucleic acids research* **1997**, *25*, 3389-3402.
[29]   J. D. Thompson, D. G. Higgins, T. J. Gibson, *Nucleic acids
         research* **1994**, *22*, 4673-4680.
[30]   E. Krieger, K. Joo, J. Lee, J. Lee, S. Raman, J. Thompson, M.
         Tyka, D. Baker, K. Karplus, *Proteins* **2009**, *77 Suppl 9*, 114-122.
[31]   K. L. Heckman, L. R. Pease, *Nat. Protocols* **2007**, *2*, 924-932.
[32]   T. Omura, R. Sato, *J. Biol. Chem.* **1964**, *239*, 2379-2385.

For internal use, please do not delete. Submitted_Manuscript

FULL PAPER

Table of Contents

FULL PAPER

Consensus guided mutagenesis was applied to stabilize the reductase domain of the biotechnologically useful P450$_{BM3}$ enzyme. The evolved variants exhibit improved robustness to thermal denaturation and increased catalytic performance at elevated temperatures.
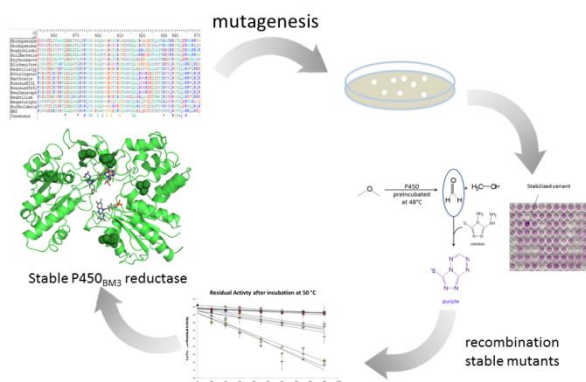
Gloria Saab-Rincón*, Hanan Alwaseem, Valeria Guzmán-Luna, Leticia Olvera and Rudi Fasan

Page No. – Page No.

Stabilization of the Reductase Domain in the Catalytically Self-Sufficient Cytochrome P450BM3 via Consensus-Guided Mutagenesis

For internal use, please do not delete. Submitted_Manuscript